Application of the cascade control method for a continuous stirred tank reactor

P. Dostál, V. Bobál, J. Vojtěšek, and B. Chramcov

***Abstract*—** The paper presents the control design of a continuous stirred tank reactor based on a combination of the cascade control and the adaptive control methologies. The control system consists of the primary a secondary control loops. The primary controlled output of the reactor is a concentration of the main reaction product, and, the secondary output is the reactant temperataure. The design of the nonlinear P-controller in the primary control loop is based on a steady-state analysis of the reactor. The controller in the secondary control-loop is an adaptive controller. The paper contains a larger number of simulations documenting suitability of the proposed method.

***Keywords*—**Adaptive control, cascade control, continuous stirred tank reactor, control simulation.

I. Introduction

CONTINUOUS stirred tank reactors (CSTRs) are equipments widely used in chemical industry, biotechnologies, polymer manufacturing, and many others. From the system theory point of view, CSTRs belong to a class of nonlinear systems with mathematical models described by sets of nonlinear differential equations as it can be seen e.g. in [1] and [2].

It is well known that the control of chemical reactors often represents very complex problem. The control problems are due to the process nonlinearity and high sensitivity of the state and output variables to input changes. One way to obtain an effective control is to use some methods of adaptive or nonlinear control. Such methods were described e.g. in [3], [4] or [5].

Another alternative is the use of a cascade control, see, e.g. [6] – [8], and its combination with the adaptive control.

In this paper, the CSTR control strategy is based on the fact that concentrations of components of reactions taking place in the reactor depend on the reactant temperature. Then, in the cascade control-loop, the concentration of a main product of the reaction is considered as the primary controlled variable, and, the reactant temperature as the secondary controlled variable. The coolant flow rate represents a common control input.

The primary control variable is measured in discrete time intervals. The primary controller determining the set point for the secondary (inner) control-loop is derived as a discrete nonlinear proportional controller using the steady-state characteristics of the reactor. Since the controlled proces is nonlinear, a continuous-time adaptive controller is used as the secondary controller. The procedure for the adaptive control design in the inner control-loop is based on approximation of the nonlinear model of the CSTR by a continuous-time external linear model (CT ELM) with recursively estimated parameters. In the process of parameter estimation, the direct identification method based on filtered control input and controlled output variables is used, see, e.g. [9] – [11].

The resulting adaptive CT controller in the 2DOF control system structure is derived using the polynomial approach and the pole placement method, see, e.g. [12] – [17].

The cascade control is verified by simulations on the nonlinear model of the CSTR.

P. Dostál, V. Bobál, J. Vojtěšek and B. Chramcov are with Faculty of Applied Informatics, Tomas Bata University in Zlin, Nad Stranemi 4511, 760 05 Zlin, Czech Republic (phone: +420 57 6035195; fax: +420 57 6035279; e-mail: {dostalp;bobal;vojtesek;chramcov}@fai.utb.cz.

II. Nonlinear Model of the CSTR

Consider a CSTR with the first order consecutive exothermic reaction according to the scheme $A \xrightarrow{k_1} B \xrightarrow{k_2} C$ and with a perfectly mixed cooling jacket. Using the usual simplifications, the model of the CSTR is described by four nonlinear differential equations

$$\frac{dc_A}{dt} = -\left(\frac{q_r}{V_r} + k_1\right)c_A + \frac{q_r}{V_r}c_{Af} \tag{1}$$

$$\frac{dc_B}{dt} = -\left(\frac{q_r}{V_r} + k_2\right)c_B + k_1 c_A + \frac{q_r}{V_r}c_{Bf} \tag{2}$$

$$\frac{dT_r}{dt} = \frac{h_r}{(\rho c_p)_r} + \frac{q_r}{V_r}(T_{rf} - T_r) + \frac{A_h U}{V_r(\rho c_p)_r}(T_c - T_r) \tag{3}$$

$$\frac{dT_c}{dt} = \frac{q_c}{V_c}(T_{cf} - T_c) + \frac{A_h U}{V_c(\rho c_p)_c}(T_r - T_c) \tag{4}$$

with initial conditions $c_A(0) = c_A^s$, $c_B(0) = c_B^s$, $T_r(0) = T_r^s$ and $T_c(0) = T_c^s$. Here, t stands for the time, c for concentrations, T for temperatures, V for volumes, ρ for densities, c_p for specific heat capacities, q for volumetric flow rates, A_h is the heat exchange surface area and U is the heat transfer coefficient. Subscripts denoted r describe the reactant mixture, c the

coolant, *f* the inlet values and the superscript *s* steady-state values.

The reaction rates and the reaction heat are expressed as

$$k_j = k_{0j} \exp\left(\frac{-E_j}{RT_r}\right),\ j = 1,2 \tag{5}$$

$$h_r = h_1 k_1 c_A + h_2 k_2 c_B \tag{6}$$

where k_0 are pre-exponential factors, E are activation energies and h are reaction entalpies. The values of all parameters, inlet values and steady-state values are given in Table 1.

TABLE I
PARAMETERS, INLET VALUES AND INITIAL CONDITIONS

V_r = 1.2 m^3 V_c = 0.64 m^3 ρ_r = 985 kg m^{-3} ρ_c = 998 kg m^{-3}	c_{pr} = 4.05 kJ kg^{-1}K^{-1} c_{pc} = 4.18 kJ kg^{-1}K^{-1} A_h = 5.5 m^2 U = 43.5 kJ m^{-2}min^{-1}K^{-1}
$k_{10} = 5.616 \cdot 10^{16}$ min^{-1} $k_{20} = 1.128 \cdot 10^{18}$ min^{-1} $h_1 = 4.8 \cdot 10^4$ kJ kmol^{-1}	E_1/R = 13477 K E_2/R = 15290 K $h_2 = 2.2 \cdot 10^4$ kJ kmol^{-1}
c_{Af}^s = 2.85 kmol m^{-3} T_{rf}^s = 323 K	c_{Bf}^s = 0 kmol m^{-3} T_{cf}^s = 293 K
q_r^s = 0.08 m^{3}min^{-1}	

The desired reaction product is a concentration of the component *B*.

III. The Control Objective

A basic scheme of the cascade control is in Fig. 1.

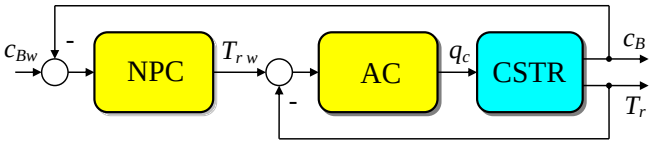

Fig. 1 Cascade control scheme.

Here, NPC stands for the nonlinear proportional controller, AC for the adaptive controller and CSTR for the reactor.

The control objective is to achieve a concentration of the component *B* as the primary controlled output near to its maximum. A dependence of the concentration of *B* on the reactant temperature is in Fig. 2.

There, an operating area consists of two parts. In the first subarea, the concentration *B* increases with increasing reactant temperature, in the second subarea it again decreases. The endpoints of the intervals defining both subareas are given as $c_B^{\min} = 0.9$, $c_B^U = 1.675$. It can be seen that the maximum value of the c_B can be slightly higher then c_B^U. However, with respect to some following procedures, the maximum desired value of c_B will be limited just by c_B^U.

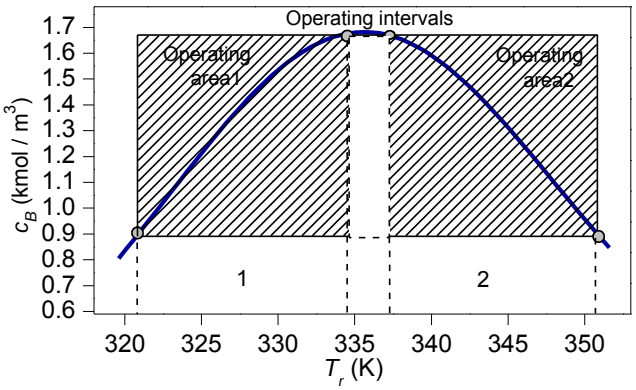

Fig. 2 Steady-state dependence of the product *B* concentration on the reactant temperature.

IV. The NPC Design

The procedure in the design of the NPC appears from inverted steady-state characteristics and its subsequent polynomial approximation.

The boundaries of operating intervals are determined as

$$0.9 \le c_B \le 1.6,\ 320.9 \le T_r \le 331.6$$

$$1.6 < c_B \le 1.675,\ 331.6 < T_r \le 334.8$$

in the first operating interval, and

$$1.675 \ge c_B > 1.6,\ 336.8 \le T_r < 339.5$$

$$1.6 \ge c_B \ge 0.9,\ 339.5 \le T_r \le 350.8$$

in the second operating interval.

For purposes of approximation, the temperature is transformed as

$$\xi = \frac{T_r - T_r^L}{T_r^U - T_r^L},\quad \xi \in \langle 0,1 \rangle \tag{7}$$

where the approximation interval is chosen a little larger than the operating interval so that $T_r^L = 319.6$ and $T_r^U = 356.0$.

Then, the polynomials approximating inverse characteristics and corresponding to above intervals then take forms

$$\xi = -0.6479 + 1.3829 c_B - 0.9588 c_B^2 + 0.2963 c_B^3 \tag{8}$$

$$\xi = 21.9485 - 27.4096 c_B + 8.686 c_B^2 \tag{9}$$

in the first operating interval, and,

$$\xi = -22.5685 + 29.2384 c_B - 9.243 c_B^2 \tag{10}$$

$$\xi = 1.6587 - 1.6398 c_B + 1.139 c_B^2 - 0.3405 c_B^3 \tag{11}$$

in the second operating interval.

Inverse characteristics together with approximations are in Figs. 3 and 4.

Now, a difference of the desired value of the reactant temperature in the output of the NPC can be computed for each c_B as

$$\Delta T_{rw} = K_w (T_r^U - T_r^L) \left(\frac{d\xi}{dc_B}\right)_{c_B} \Delta c_{Bw} \tag{12}$$

where $\Delta c_{Bw} = c_{Bw} - c_B^s$, $\Delta T_{rw} = T_{rw} - T_r^s$, and K_w is a selectable gain coefficient.

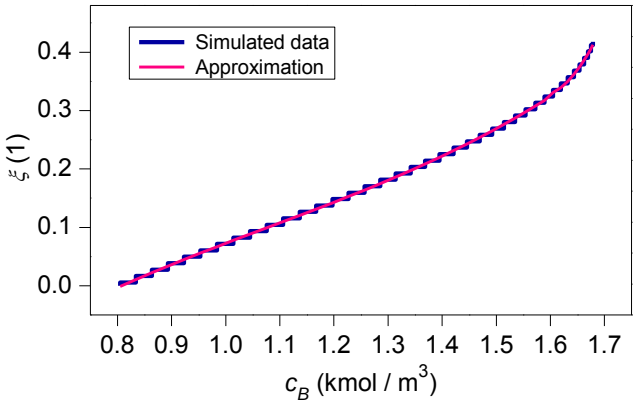

Fig.3 Inverse steady-state characteristics in the interval 1.

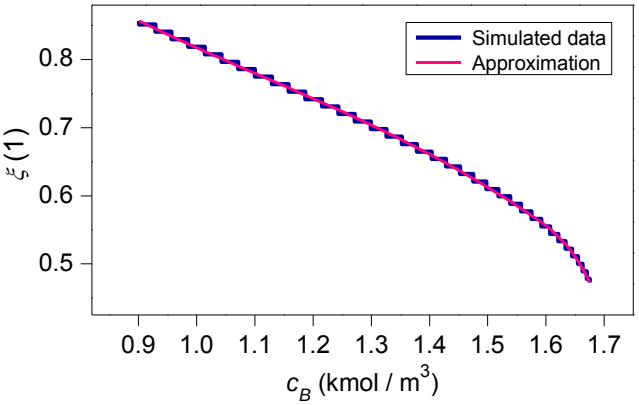

Fig.4 Inverse steady-state characteristics in the interval 2.

Formulas for computing of derivatives corresponding to (8) – (11) are

$$\frac{d\xi}{dc_B} = 1.3829 - 1.9176\,c_B + 0.8888\,c_B^2 \tag{13}$$

$$\frac{d\xi}{dc_B} = -27.4096 + 17.3714\,c_B \tag{14}$$

in the first operating interval, and,

$$\frac{d\xi}{dc_B} = 29.2384 - 18.4859\,c_B \tag{15}$$

$$\frac{d\xi}{dc_B} = -1.6398 + 2.2781\,c_B - 1.0216\,c_B^2 \tag{16}$$

in the second operating interval.

Note that the maximal desired value c_{Bw} is chosen in all cases as $c_{Bw} \le 1.675$.

V. Adaptive Control System Design

The nonlinearity of the reactor is evident from the shape of the dependence T_r on q_c in the steady-state shown in Fig. 5.

A. External Linear Model of the CSTR

For the control purposes, the controlled output and the control input are defined as

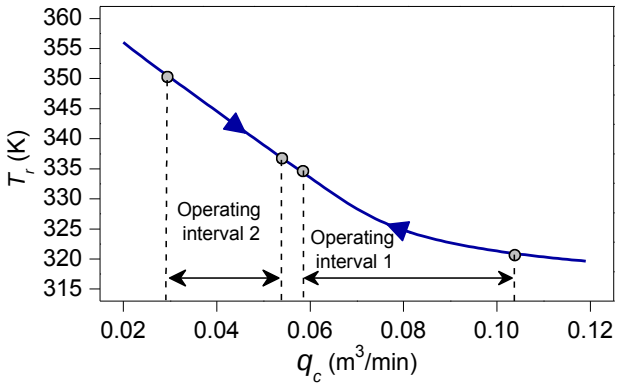

Fig. 5 Steady-state characteristics $T_r^s - q_c^s$ of the CSTR.

$$y(t) = \Delta T_r(t) = T_r(t) - T_r^s,\ u(t) = q_c(t) - q_c^s \tag{17}$$

The CT ELM is proposed in the time domain on the basis of simulated step responses shown in Fig. 6 in the form of the second order differential equation

$$\ddot{y}(t) + a_1\dot{y}(t) + a_0 y(t) = b_0 u(t) \tag{18}$$

and, in the complex domain as

$$(s^2 + a_1 s + a_0)Y(s) = b_0 U(s)$$

$$G(s) = \frac{b(s)}{a(s)} = \frac{b_0}{s^2 + a_1 s + a_0} \tag{19}$$

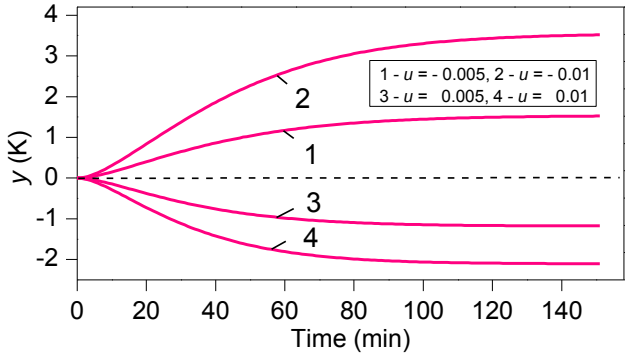

Fig. 6 Controlled output step responses.

B. CT ELM Parameter Estimation

The method of the CT ELM parameter estimation can be briefly carried out as follows.

Since the derivatives of both input and output cannot be directly measured, filtered variables u_f and y_f are established as the outputs of filters

$$c(\sigma)u_f(t) = u(t) \tag{20}$$

$$c(\sigma)y_f(t) = y(t) \tag{21}$$

where $\sigma = d/dt$ is the derivative operator, $c(\sigma)$ is a stable polynomial in σ that fulfills the condition $\deg c(\sigma) \ge \deg a(\sigma)$.

Note that the time constants of filters must be smaller than the time constants of the process. Since the latter are unknown at the beginning of the estimation procedure, it is necessary to

make the filter time constants, selected a priori, sufficiently small.

With regard to (19), the polynomial *a* takes the concrete form $a(\sigma)=\sigma^2+a_1\sigma+a_0$, and, the polynomial *c* can be chosen as $c(\sigma)=\sigma^2+c_1\sigma+c_0$. Subsequently, the values of the filtered variables can be computed during the control by a solution of (20) and (21) using some standard integration method.

It can be easily proved that the transfer behavior among filtered and among nonfiltered variables are equivalent. Using the *L*-transform of (20) and (21), the expressions

$$c(s)U_f(s)=U(s)+\mu_1(s) \tag{22}$$

$$c(s)Y_f(s)=Y(s)+\mu_2(s) \tag{23}$$

can be obtained with μ_1 and μ_2 as polynomials of initial conditions. Substituting (22) and (23) into (19), and, after some manipulations, the relation between transforms of the filtered input and output takes the form

$$Y_f(s)=\frac{b(s)}{a(s)}U_f(s)+M(s)=G(s)U_f(s)+M(s) \tag{24}$$

where $M(s)$ is a rational function as the transform of any function $\mu(t)$ which expresses an influence of initial conditions of filtered variables.

Now, the filtered variables including their derivatives can be sampled from filters (20) and (21) in discrete time intervals $t_k = k\,T_S$, k = 0,1,2, ... where T_S is the sampling period. Denoting deg $a = n$ and deg $b = m$, the regression vector is defined as

$$\begin{aligned}\boldsymbol{\Phi}(t_k)=\big[&-y_f(t_k)-y_f^{(1)}(t_k)\ldots-y_f^{(n-1)}(t_k)\\ &u_f(t_k)\,u_f^{(1)}(t_k)\ldots u_f^{(m)}(t_k)\;\;1\big]\end{aligned} \tag{25}$$

Now, the vector of parameters

$$\boldsymbol{\Theta}^T(t_k)=\big[a_0\;a_1\;\ldots\;a_{n-1}\;b_0\;b_1\ldots\;b_m\big] \tag{26}$$

can be estimated from the ARX model

$$y_f^{(n)}(t_k)=\boldsymbol{\Theta}^T(t_k)\Phi(t_k)+\mu(t_k) \tag{27}$$

Here, the recursive identification method with exponential and directional forgetting was used according to [18].

C. Controller Design

For the adaptive control purposes, the 2DOF controller is used. It is known that this type of the controller often provides smoother control actions then a standard feedback controller. The 2DOF controller consist of the feedback part *Q* and the feedforward part *R* as shown in Fig. 7.

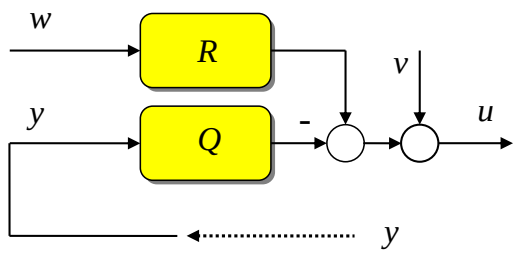

Fig. 7 The 2DOF controller.

In the scheme, *w* is the reference signal $w=T_{rw}-T_r^s$, *y* is the controlled output and *u* the control input to the CSTR. The reference *w* and the disturbance *v* are taken into account as sequences of step functions with transforms

$$W_k(s)=\frac{w_{k0}}{s}\,,\quad V_k(s)=\frac{v_{k0}}{s} \tag{28}$$

The transfer functions of both controller parts are in forms

$$R(s)=\frac{r(s)}{p(s)},\quad Q(s)=\frac{q(s)}{p(s)} \tag{29}$$

where *q*, *r* and *p* are coprime polynomials in *s* fulfilling the condition of properness $\deg r\le\deg p$ and $\deg q\le\deg p$. For a step disturbance with the transform (28), the polynomial *p* takes the form $p(s)=s\,\tilde{p}(s)$.

The controller design described in this section follows from the polynomial approach. It is known that an admissible controller ensuring stability and internal properness of the control system, asymptotic tracking of the reference and disturbance attenuation results from a solution of the couple of polynomial equations

$$a(s)s\,\tilde{p}(s)+b(s)q(s)=d(s) \tag{30}$$

$$t(s)s+b(s)r(s)=d(s) \tag{31}$$

with a stable polynomial *d* on their right sides. The polynomial $t(s)$ is an auxiliary polynomial which does not enter into the controller design but it is necessary for calculation of (31).

For the transfer function (19) with deg a = 2, the controller transfer functions take forms

$$\begin{aligned}Q(s)&=\frac{q(s)}{s\,\tilde{p}(s)}=\frac{q_2s^2+q_1s+q_0}{s(s+p_0)}\\ R(s)&=\frac{r(s)}{s\,\tilde{p}(s)}=\frac{r_0}{s(s+p_0)}\end{aligned}\,. \tag{32}$$

Moreover, the equality $r_0=q_0$ can easily be obtained.

The controller parameters then follow from solutions of polynomial equations (30) and (31) and depend upon coefficients of the polynomial *d*.

In this paper, the polynomial *d* with roots determining the closed-loop poles is chosen as

$$d(s)=n(s)(s+\alpha)^2 \tag{33}$$

where *n* is a stable polynomial obtained by spectral factorization

$$a^*(s)a(s)=n^*(s)n(s) \tag{34}$$

and α is the selectable parameter that can usually be chosen by way of simulation experiments. Note that a choice of *d* in the form (33) provides the control of a good quality for aperiodic controlled processes. The polynomial *n* has the form

$$n(s)=s^2+n_1s+n_0 \tag{35}$$

with coefficients

$$n_0=\sqrt{a_0^2}\,,\quad n_1=\sqrt{a_1^2+2n_0-2a_0}\,. \tag{36}$$

The controller parameters can be obtained from solution of the matrix equation

$$\begin{pmatrix} 1 & 0 & 0 & 0 \\ a_1 & b_0 & 0 & 0 \\ a_0 & 0 & b_0 & 0 \\ 0 & 0 & 0 & b_0 \end{pmatrix} \cdot \begin{pmatrix} p_0 \\ q_2 \\ q_1 \\ q_0 \end{pmatrix} = \begin{pmatrix} d_3 - a_1 \\ d_2 - a_0 \\ d_1 \\ d_0 \end{pmatrix} \tag{37}$$

where

$$d_3 = n_1 + 2\alpha,\ d_2 = 2\alpha n_1 + n_0 + \alpha^2$$
$$d_1 = 2\alpha n_0 + \alpha^2 n_1,\ d_0 = \alpha^2 n_0 \tag{38}$$

Evidently, the controller parameters can be adjusted by the selectable parameter α.

VI. Simulation Results

Consider the measurement of the concentration c_B in periods t_B (min). The aim of simulations is to show an effect of this period, an effect of the parameter K_w and an effect of the selectable pole α on some control responses.

For the CT ELM parameter recursive identification, the sampling period T_s = 1 min has been chosen. Values of the filter parameters were chosen as $c_1 = 1.5$, $c_0 = 0.5$.

For the start (the adaptation phase), the P controller with a small gain was used in all simulations.

The first part of simulations started at the starting point $c_B^s = 1.2$, $T_r^s = 324.8$ and $q_c^s = 0.08$ in the first operating area, and, at $c_B^s = 0.9$, $T_r^s = 350.8$ and $q_c^s = 0.029$ in the second operating area. Values of used parameters are stated under each figure.

An effect of the parameter K_w on the control responses in the first operating area is evident from Figs. 8 – 10. An increasing K_w accelerates all signals in the control loop. However, its value is not unrestricted and its convenient value should be found experimentally.

An effect of the period t_B in the same operating interval can be seen in Figs. 11 – 13. Although shortening t_B leads to faster control responses, its length is determined by possibilities of measurement.

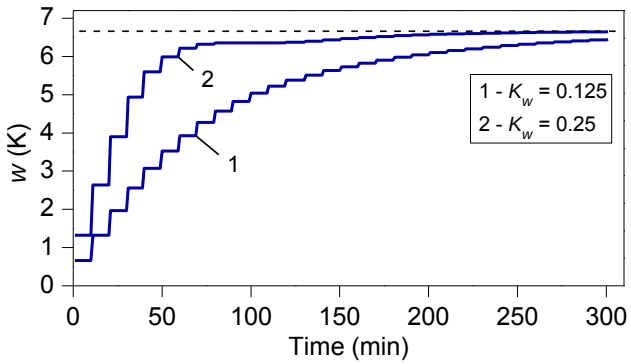

Fig. 8 Reference signal courses (t_B = 10, α = 0.2).

An influence of the selectable pole α on the reference signal, the reactant temperature and the output concentration responses is documented by simulations in Figs. 14 – 16. It can be seen that there is not a significant difference between results obtained by both choices of α.

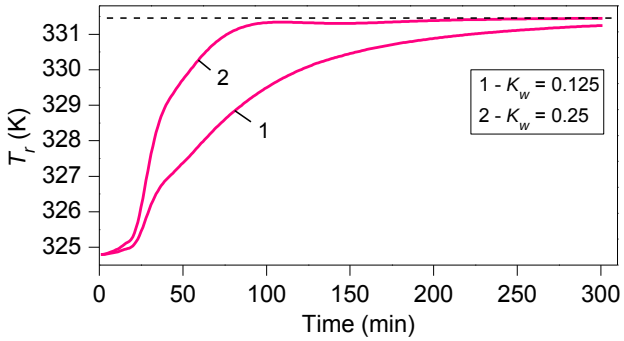

Fig. 9 Reactant temperature responses (t_B = 10, α = 0.2).

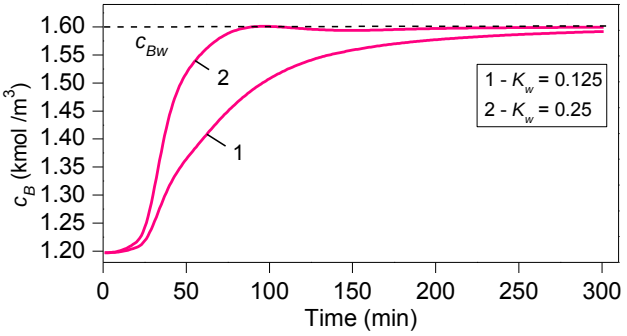

Fig. 10 Concentration c_B responses (t_B = 10, α = 0.2).

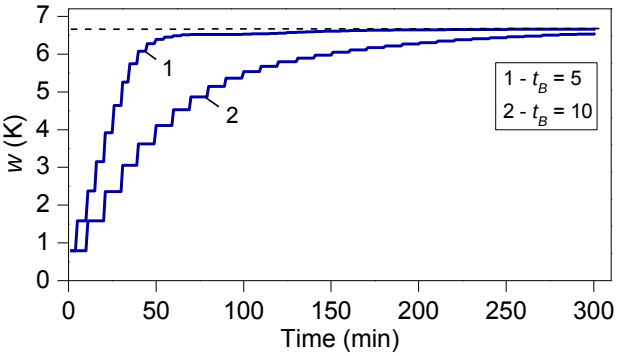

Fig. 11 Reference signal courses (K_w = 0.15, α = 0.2).

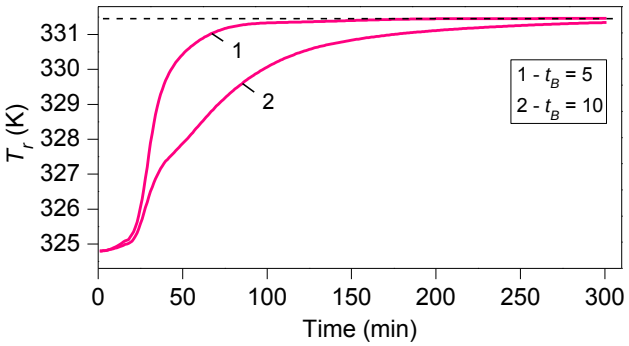

Fig. 12 Reactant temperature responses (K_w = 0.15, α = 0.2).

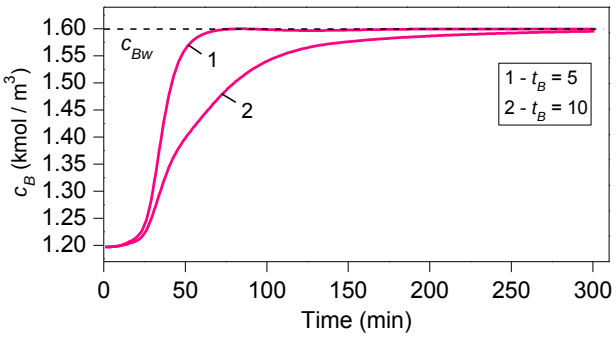

Fig. 13 Concentration c_B responses (K_w = 0.15, α = 0.2).

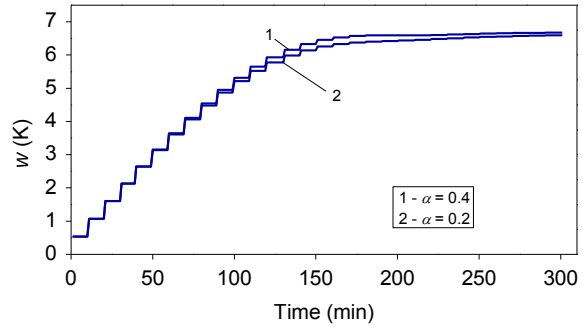

Fig. 14 Reference signal courses (K_w = 0.1, t_B = 10).

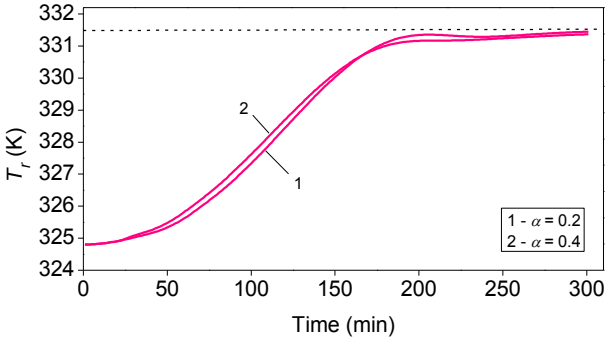

Fig. 15 Reactant temperature responses (K_w = 0.1, t_B = 10).

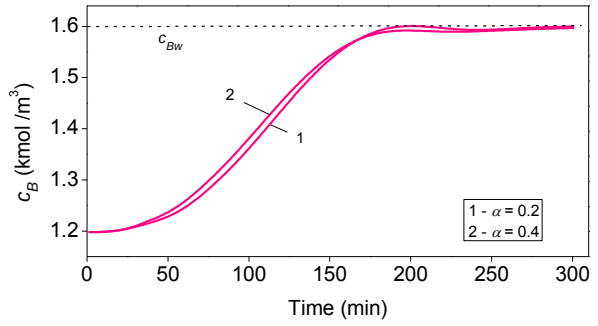

Fig. 16 Concentration c_B responses (K_w = 0.1, t_B = 10).

The reference signal courses, the reactant temperature and the concentration c_B responses simulated in the second operating area are shown in Figs. 17 – 19. Here it can be seen a high sensitivity to the controller gain. On the basis of simulation experiments it can be recommended to chose rather its less value. For illustration, the coolant flow rate courses are shown in Fig. 20.

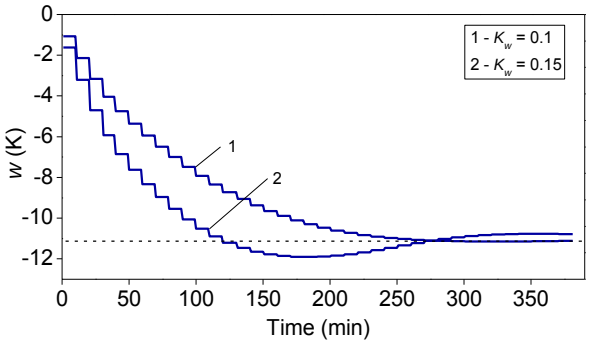

Fig. 17 Reference signal courses (t_B = 10, α = 0.4).

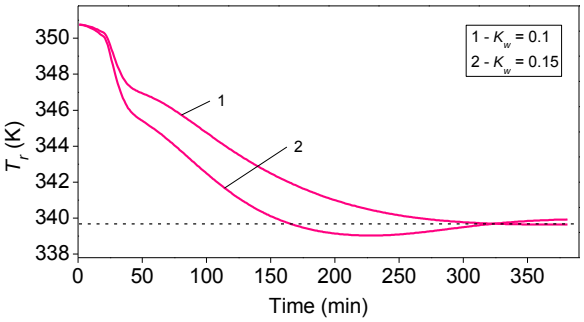

Fig. 18 Reactant temperature responses (t_B = 10, α = 0.4).).

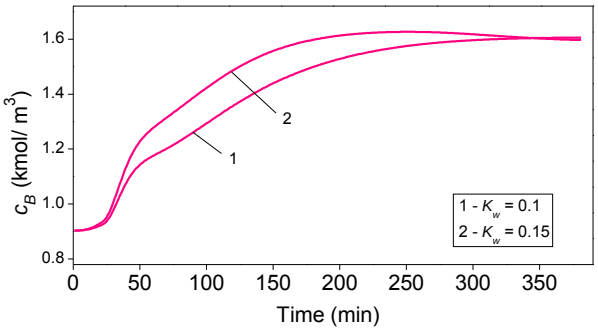

Fig. 19 Concentration c_B responses (t_B = 10, α = 0.4).

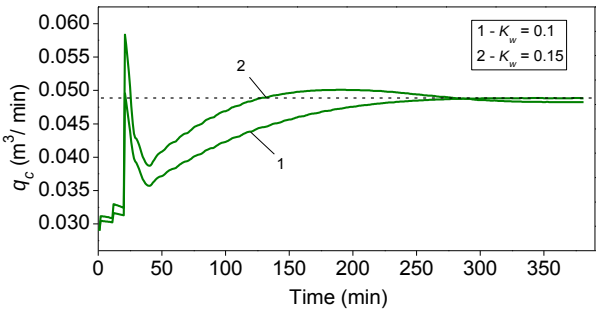

Fig. 20 Coolant flow rate response (t_B = 10, α = 0.4).

The courses of signals during transitions between

approximations (8) and (9) in the first operating interval, and, between approximations (10) and (11) in the second operating interval are in Figs. (21) – (26). Starting steady-state values were chosen as $c_B^s = 1.443$ kmol/m^3, $T_r^s = 328.4$ K in the first operating interval, and, $c_B^s = 1.024$ kmol/m^3, $T_r^s = 349.06$ K in the second operating interval. The desired value $c_{Bw} = 1.675$ kmol/m^3 has been chosen in both cases.

All simulated signal responses including the coolant flow rate response in Fig. 27 documente suitability of the proposed procedure.

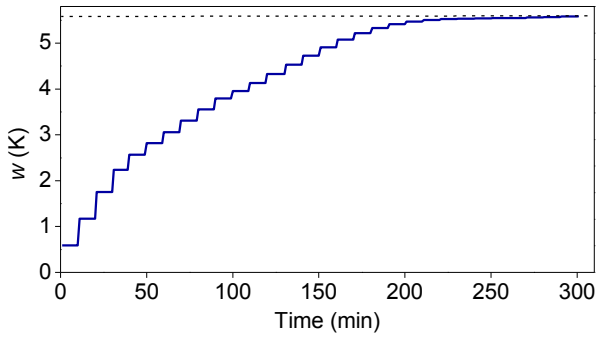

Fig. 21 Reference signal course (K_w = 0.15 t_B = 15, α = 0.2).

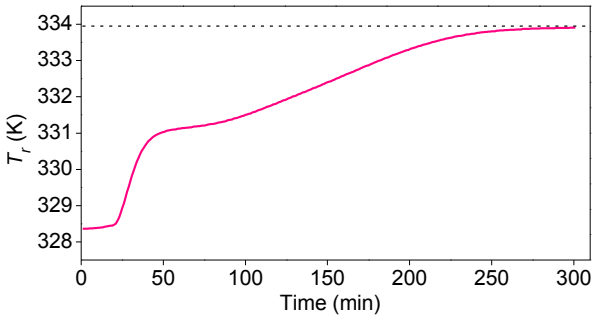

Fig. 22 Reactant temperature response (K_w = 0.15 t_B = 15, α = 0.2).

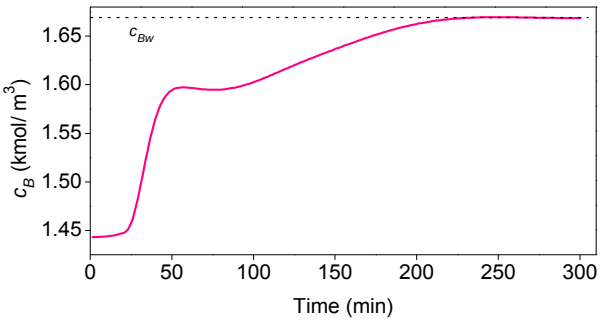

Fig. 23 Concentration c_B response (K_w = 0.15 t_B = 15, α = 0.2).

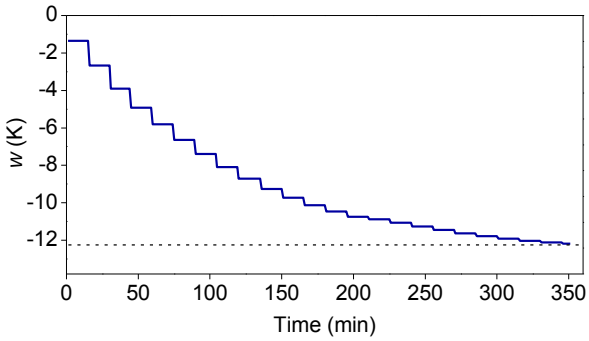

Fig. 24 Reference signal course (K_w = 0.15 t_B = 10, α = 0.4).

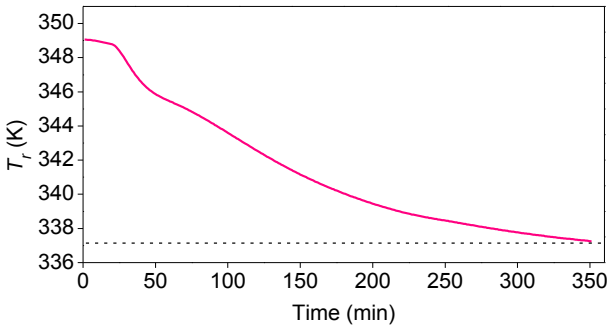

Fig. 25 Reactant temperature response (K_w = 0.15 t_B = 10, α = 0.4).

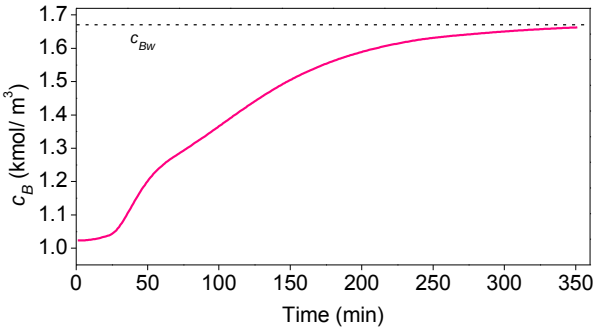

Fig. 26 Concentration c_B response (K_w = 0.15 t_B = 10, α = 0.4).

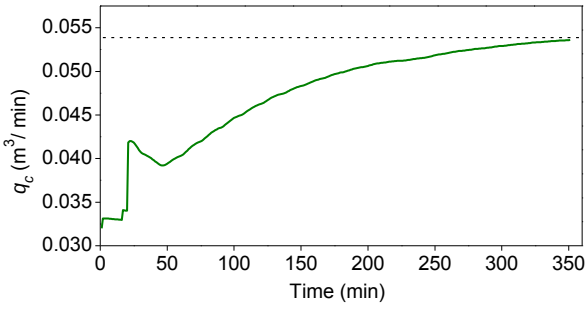

Fig. 27 Coolant flow rate response (K_w = 0.15 t_B = 10, α = 0.4).

VII. Conclusions

The subject of the article is the cascade control design of a continuous stirred tank reactor. A necessary condition for the use of the presented method is measurement of a main product of the reaction taking place in the reactor. The control is performed in the external (primary) and inner (secondary) closed-loop where the concentration of a main product is the primary and the reactant temperature the secondary controlled variable. A common control input is the coolant flow rate.

The controller in the external control-loop is a discrete nonlinear P-controller derived on the basis of approximations of inverse steady-state characteristics of the reactor and their derivatives. The controller in the inner control-loop is a 2DOF adaptive continuous-time controller. In its derivation, the recursive parameter estimation, the polynomial approach and the pole placement method were applied.

The control was tested by simulations on the nonlinear model of the CSTR.

REFERENCES

[1] R. Smith, *Chemical process design and integration*. Chichester: John Wiley and Sons, 2005.

[2] J.-P. Corriou, *Process control. Theory and applications*. London: Springer – Verlag, 2004.

[3] Chen1, Chyi-Tsong, Chuang1, Yao-Chen, and Hwang, Chyi, "A simple nonlinear control strategy for chemical processes," in *Proc. 6th Asian Control Conference*, Bali, Indonesia, 2006, pp. 64-70.

[4] P. Dostál, V.Bobál, F. Gazdoš, "Simulation of nonlinear adaptive control of a continuous stirred tank reactor," *International Journal of mathematics and computers in simulation*, vol. 5, 2011, pp. 370-377.

[5] A. Astolfi, D. Karagiannis, and R. Ortega, *Nonlinear and adaptive control with applications*. London: Springer-Verlag, 2008.

[6] D.E. Seborg, T.F. Edgar, and D.A. Mellichamp, *Process dynamics and control*. Chichester: John Wiley and Sons, 1989.

[7] J.F. Smuts, *Process control for practitioners*. New York: OptiControls, 2011.

[8] M. Morari, and E. Zafiriou, *Robust process control*. New York: Prentice Hall, 1989.

[9] G.P. Rao, and H. Unbehauen, "Identification of continuous-time systems," *IEE Proc.-Control Theory Appl*., vol. 153, 2006, pp. 185-220.

[10] H. Garnier, and L. Wang (eds.), *Identification of continuous-time models from sampled data*, London: Springer-Verlag, 2008.

[11] P. Dostál, V. Bobál, and F. Gazdoš, "Adaptive control of nonlinear processes: Continuous-time versus delta model parameter estimation," in *Proc. 8th IFAC Workshop on Adaptation and Learning in Control and Signal Processing ALCOSP 04*, Yokohama, Japan, 2004, pp. 273-278.

[12] M.J. Grimble, *Robust industrial control*. *Optimal design approach for polynomial systems*. London: Prentice Hall, 1994.

[13] V. Kučera, "Diophantine equations in control – A survey," *Automatica*, vol. 29, 1993, pp. 1361-1375.

[14] W.L. Brogan, *Modern control theory*. New Jersey, Prentice Hall, 1991.

[15] G.F. Franklin, J.D. Powell, and A. Emami-Naeini, *Feedback control of dynamic systems*. New Jersey: Pearson Prentice Hall, 2006.

[16] P. Dostal, J. Vojtesek, and V. Bobal, "Adaptive LQ control of a shell and tube heat exchanger," *International Journal of Mathematics and Computers in Simulation*, vol. 7, 2013, pp. 389-397.

[17] P. Dostál, V. Bobál, J. Vojtěšek, and Z. Babík, "One approach to adaptive control of a tubular chemical reactor," *WSEAS Transactions on Fluid Mechanics*, vol. 7, 2012, pp. 13-22,

[18] V. Bobál, J. Böhm, J. Fessl, and J. Macháček, *Digital self-tuning controllers*, Berlin: Springer Verlag, Berlin, 2005.